Journal of Mechatronics, Electrical Power, and Vehicular Technology 15 (2024) 42-56

Journal of Mechatronics, Electrical Power, and Vehicular Technology

e-ISSN: 2088-6985
p-ISSN: 2087-3379

mev.brin.go.id

Photovoltaic energy harvesting booster under partially shaded conditions using MPPT based sand cat swarm optimizer

Moch Rafi Damas Abdilla *, Novie Ayub Windarko, Bambang Sumantri

Electrical Engineering Department, Politeknik Elektronika Negeri Surabaya
Jalan Raya ITS Sukolilo Kampus PENS, Surabaya, 60111, Indonesia

Abstract

Photovoltaic (PV) systems perform a vital role in addressing the worldwide energy crisis and fulfilling the escalating energy demand. The variability in irradiance, temperature, and unpredictable weather conditions possess a direct impact on the productivity of PV systems. Furthermore, the existence of partially shaded conditions intensifies the complexity of PV systems, resulting in significant power degradation. These conditions present significant challenges for PV systems to achieve maximum power output and produce optimal energy. To address the prevailing challenges, this study introduces a maximum power point tracking (MPPT) control methodology utilizing a sand cat swarm optimizer (SCSO). This ingenious strategy adapts the sand cat hunting style. The investigation centers on optimizing energy harvesting in PV systems, with a specific emphasis on enhancing precision, rapid convergence, and minimizing oscillations. The suggested SCSO performance is evaluated under a variety of weather situations, including both instances of partially shaded and uniform irradiance. The SCSO results are juxtaposed with other existing bio-inspired algorithms, such as grey wolf optimization (GWO), particle swarm optimization (PSO), and tunicate swarm algorithm (TSA). The proposed SCSO technique achieves 99.94 % tracking accuracy on average and shows superior performance, with faster tracking response and less power oscillation. Moreover, the proposed SCSO generates significantly more energy than the rest compared algorithms. The performance of the suggested method is further validated through a hardware-based experimental assessment, demonstrating an optimal level of tracking performance.

Keywords: energy harvesting; maximum power point tracking (MPPT); partially shaded conditions; photovoltaic (PV) system; sand cat swarm optimization (SCSO).

I. Introduction

The world currently faces a critical challenge in the guise of warming climates, which presents a substantial danger to the worldwide economy, the natural environment, and the sustenance of human life. This pressing issue is primarily driven by an increasing concentration of greenhouse emissions in the Earth's atmosphere, largely resulting from human events such as the combustion of fossil fuels, industrialization, and urban development [1]. Due to increasing world energy demand and rising fossil fuel prices along with growing concern about environmental issues, governments and researchers worldwide have recognized the urgency of addressing this problem and have initiated investments in renewable energy sources and the development of green technologies.

Among these renewable energy sources, solar energy stands out as one of the most promising solutions to our energy needs [2]. Solar photovoltaic

* Corresponding Author. rafidamas1@gmail.com (M. R. D. Abdilla)

https://doi.org/10.55981/j.mev.2024.857

Received 1 February 2024; 1st revision 21 March 2024; 2nd revision 1 April 2024; 3rd revision 5 April 2024; accepted 18 April 2024; available online 31 July 2024

How to Cite: M. R. D. Abdilla, N. A. Windarko, B. Sumantri, "Photovoltaic energy harvesting booster under partially shaded conditions using MPPT based sand cat swarm optimizer," *Journal of Mechatronics, Electrical Power, and Vehicular Technology*, vol. 15, no. 1, pp. 42-56, July 2024.

(PV) systems have gained substantial attention due to their effortless installation, abundant sunlight availability, low maintenance costs, and silent characteristic [3]. These devices utilize the photoelectric effect to capture and convert solar energy into electrical power. However, despite extensive schemes to enhance the productivity of PV systems, they still face substantial challenges and limitations, particularly related to their nonlinear characteristics and poor efficiency in converting energy [4]. One of the major challenges associated with PV systems is their dependency on atmospheric conditions, such as temperature and radiation levels, which continually change throughout the day. The complexity of this task becomes even more complex when partial shading occurs, a situation which refers to the unequal distribution of solar radiation across the PV system due to obstructions like clouds, trees, and buildings in the nearby area [5][6]. It generates multiple maximum power point (MPP) with global maximum power point (GMPP) as the peak power, and the lower power point is local maximum power point (LMPP) [7]. Thus, the generated power of PV decreases significantly, resulting in a substantial amount of energy being inefficiently dissipated.

To address these challenges and improve the efficiency of PV systems, special controllers known as maximum power point tracking (MPPT) controllers are employed [8]. The MPPT controller plays a crucial function in a PV system by effectively optimizing power generation and efficiency. The controllers, which are commanded by advanced control algorithms, are responsible for regulating the duty cycle of the DC-DC converter to accurately follow the GMPP under varying atmospheric conditions. Various classic conventional MPPT techniques have been introduced over the years, among them perturb and observe (P&O) [9], incremental conductance (INC) [10], and hill-climbing (HC) [11]. While these methods are relatively simple and easily accessible, they suffer some challenges like power oscillation, poor convergence time, and the risk of failure in achieving GMPP when exposed to rapidly fluctuating irradiance or partially shaded circumstances [12]. As a result of these deficiencies, the energy harvested is extremely inefficient and very small. Some improvements have been made by applying a variable step size instead of a constant step size, which enhanced power amount and tracking speed. However, it didn't fully address the oscillation problem and often increased algorithm complexity.

Researchers have placed forward multiple types of bio-inspired algorithms as a reaction to the problems found in conventional methods [13]. For instance, particle swarm optimization (PSO) was proposed by many researchers. It makes PSO the most frequently used algorithm for PV MPPT [14]. While the PSO algorithm demonstrated precision in attaining the MPP and remained stable under consistent radiation conditions, it encountered difficulties in achieving swift convergence when faced with fluctuating radiation conditions and presented implementation challenges in real-world scenarios [15][16]. Others, grey wolf optimization (GWO), have demonstrated abilities in MPPT [17]. However, these algorithms have been hindered by complex functions and long processing times, making the physical hardware system challenging.

Reference [18], the falcon optimization algorithm (FOA) has been shown to be effective in GMPP tracking with promising accuracy and low energy losses. However, it can suffer from inadequate performance if it is not properly initialized or tuned. Moreover, FOA has a high computational cost and it can be slow to converge on complex problems [19]. Reference [20], a tunicate swarm algorithm-based MPPT control is introduced. This algorithm models the tunicate's talent to find food in the sea using their jet propulsion to move and record the best position. The simulation findings demonstrate the ability of good tracking in various climate situations. However, the main drawbacks are the protracted convergence speed and the strong influence of the initial position. Recently, an innovative approach involved the reptile search optimizer (RSA) method, which was proposed with a sequential update mechanism. RSA demonstrated robustness, strong potency, and adaptive capabilities in tracking the MPP of the system. However, RSA MPPT still has some limitations including steady-state oscillations, difficulties in parameter initialization, and the practical implementation [21].

After a comprehensive assessment of these published algorithms, it became evident that while many of them proved successful in conducting GMPP, they occasionally underperformed in certain circumstances by being taken at LMPP. The performance of these algorithms depended on the complex configuration of the PV system and the environmental conditions. From this perspective, there is a consistent encouragement to enhance the performance of MPPT by inventing or implementing a novel intelligent algorithm that exhibits greater prospects for MPPT application.

Following a thorough literature research on the newly introduced intelligent optimization algorithms, sand cat swarm optimizer (SCSO) algorithm has been noted due to its easy implementation, fewer mathematic models, adaptive capabilities, and notable design [22]. SCSO has a unique method inspired of the

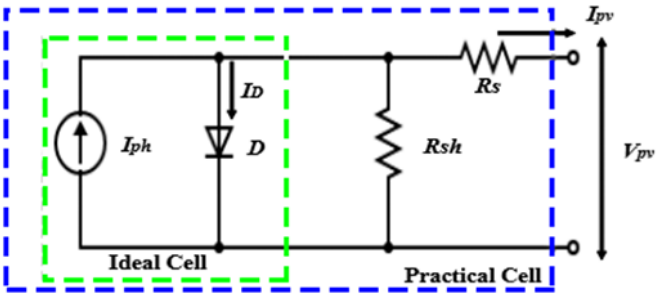

Figure 1. Single-diode PV equivalent circuit model.

Table 1.
PV parameter.

Parameter	Value
Number of cells	36
Rated maximum power (P_{max})	100 W
Voltage at max (V_{mp})	17.8 V
Current at max (I_{mp})	5.62 A
Open-circuit voltage (V_{oc})	21.8 V
Short-circuit current (I_{sc})	6.05 A
Standard test condition	1000 W/m^2; 25 °C

noise detection behavior of sand cats to find prey. The sand cats have a wide auditory range, which makes them detect low frequencies signal below 2 kHz. This hearing talent ensures that sand cats have a special ability to search and hunting in nature. The mechanisms are allowing the algorithm to preserve diversity among potential solutions while identifying the optimal one. Moreover, it ensures to balanced behavior between exploitation and exploration. Compared to the general cats which inspire a cat swarm optimizer (CSO), CSO emphasizes cat hunting strategies of seeking and tracking, which translates into more general exploration-exploitation [23]. In contrast, SCSO's focus on mimicking sand cat hunting through sound localization introduces a more balanced and targeted exploration-exploitation mechanism, making it potentially faster at converging toward good solutions [24]. The proposed SCSO algorithm can efficiently track the global solution and avoids local optima with a swift tracking time and slight power fluctuation. The advancements of the SCSO algorithm are essential to boosting the harvested energy of PV systems, thus contributing to the broader goal of reducing greenhouse gas emissions and mitigating global warming.

II. Materials and Methods

A. Photovoltaic system

A general equivalent circuit of a single-diode PV panel model is shown in Figure 1. It contains of current source parallel connected with a diode and resistor shunt, then connected with a series resistor at the output terminal. According to the PV equivalent circuit, the I - V characteristic of the PV panel is given in equation (1). I_{ph} current which is a PV current generated from the converting process of solar energy into electrical energy, is given in equation (2) [25].

$$I_{pv} = I_{ph} - I_{sat}\left[e^{\frac{q\cdot(V_{pv}+R_S\cdot I_{pv})}{a\cdot k\cdot T}} - 1\right] - \frac{V_{pv}+R_S\cdot I_{pv}}{R_{sh}} \quad (1)$$

$$I_{ph} = \frac{G}{G_n}[I_{sc} + k(T - T_n)] \quad (2)$$

where I_{pv} is the output current (A) and V_{pv} is the output voltage (V) at the output terminal, which is directly connected to the load. I_{sat} is the saturation current (A), I_{ph} is PV current (A), R_s and R_{sh} are series resistor and parallel resistor of PV panel (Ω), q is electron capacity or electron charge (1.6×10^{-19} C), k is Boltzmann's constant ($1.3806503 \times 10^{-23}$ J/K), a is the ideal diode factor. Then, I_{sc} is the short circuit current of PV panel (A) in the standard test condition (STC), G is irradiation received by the PV panel (W/m^2), G_n is irradiation in the STC (1000 W/m^2), T is cell temperature (K), and T_n is the temperature in the STC (298.15 K). PV panels used for this system are ST-Solar Polycrystalline 100 Wp. The parameter of this panel is shown in Table 1.

The amount of power generated is greatly influenced by the level of solar irradiation. It can be stated that the power generated is proportionate to the radiation value. The PV exhibits a non-linear characteristic of power and voltage. Under partially shaded array conditions, the shaded panel produces

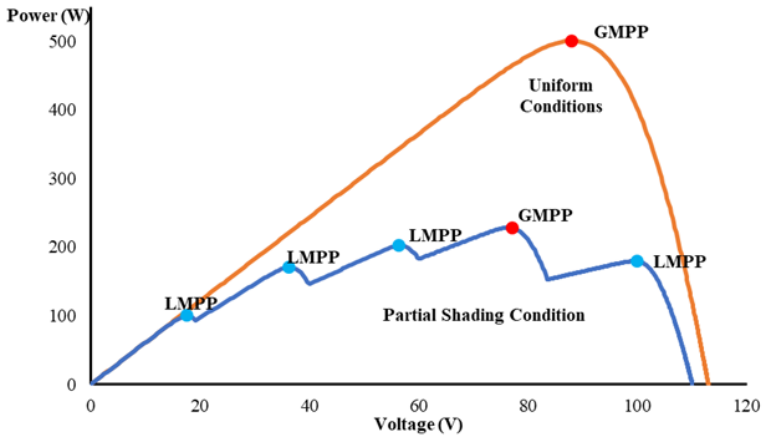

Figure 2. PV characteristic.

lower energy than the non-shaded panel. It exhibits multiple peak points. Figure 2 displays the characteristics of the PV under different conditions. The lower peaks are denoted as LMPP, whereas the highest point is identified as GMPP.

B. DC-DC boost converter

Boost converter acting as MPPT controller to operate the PV array at the objective value and produce the highest power. The DC-DC converter used for this paper is a DC-DC boost converter, which is it affords to generate higher output voltage during lower output current. For obtaining the GMPP of PV panels, the duty cycle of the DC-DC converter is changed by the MPPT algorithm. Changes in the duty cycle can make the output voltage and current of the PV vary to get the GMPP value. The parameter of the boost converter is obtained from equation (3) to equation (6) [26]:

$$V_o = \frac{V_{in}}{1-D} \tag{3}$$

$$D = \frac{T_{on}}{T_s} \tag{4}$$

$$L_{min} = \frac{D(1-D)^2 R}{2 \cdot f} \tag{5}$$

$$C = \frac{D}{R \cdot f \cdot rV_o} \tag{6}$$

where V_{in} denoting the input voltage from the PV panels (V), while the converter output voltage is represented as V_o (V), D indicated the duty cycle (%), T_{on} refers to the switching is turned on (s), T_s as the switching period (s). L_{min} signifies the minimal inductance value (H), while operating in continuous current mode (CCM). Then, R stands for load resistance (Ω), f is switching frequency (Hz), C symbolizes the capacitance value (F), rV_o be present the ripple output voltage of the converter (%). Notably, the system targets a 0.1 % value for the ripple output voltage. The corresponding parameter values for the boost converter are summarized in Table 2.

C. Sand cat swarm optimizer

The SCSO algorithm was inspired by the surviving behavior and unique characteristics of sand cat in nature. Sand cat is known to inhabit desert areas characterized by sandy and rocky deserts, including the Arabian Peninsula and Sahara. They eat small desert animals, tiny reptiles, snakes, and flying insects. The surviving behavior of sand cat is different than domestic cat. Despite their similar physical characteristics, sand cats possess a broader hearing range. Which enables them to detect and respond to low-frequency sounds under 2 kHz, even the prey below the sand surface. It makes the sand cat find and attack their food rapidly [27].

The hunting mechanism of the sand cat, characterized by searching and attacking, became the inspiration for the mathematical modeling of the SCSO algorithm. The search procedure necessitates agents to traverse a broad expanse, which is also referred to as the exploration phase. Then, the attack procedure allows them to get the prey with a quick move and effectively. It is called exploitation. These processes generate a new

Table 2.
Component value of the boost converter.

Component	Value
Capacitor	1.2 µF
Inductor	571 µH
Resistor load	60 Ω
Switching frequency	20 kHz

position for each sand cat, where the position represents the duty cycle value of the converter.

The search process, as the exploration phase, obliges agents to prowl over a wide area. The search area is generated randomly around the limited defined area. The formula of searching is described in equation (7)

$$X(it+1) = r \cdot (X_{best} - rand \cdot X_{current}) \quad (7)$$

$$r = r_G \cdot rand \quad (8)$$

$$r_G = S_M - \left(\frac{S_M * it}{Max\ it}\right) \quad (9)$$

where X is position of sand cat, it is iteration, Max it is maximum iteration, $X(it+1)$ is the updated position, X_{best} is the best position, $X_{current}$ is current position of cat, $rand$ is random number from 0 to 1, r simulates the hearing sensitivity of cats as modeled in equation (8), and S_M is the maximum sensitivity range with a value of 2. The sensitivity range, r_G, is updated using equation (9).

After they locate the prey position, sand cat attacks their prey quickly. The new position was exploiting around the best solution so far. The movement is determined by random angle (θ). The attacking mechanism is modeled in equation (10) where θ is a circular random angle, X_{rand} is a random position as calculated by equation (11). Each cat has a different angle, which aims to get the optimal position and avoid getting trapped in the local optimal.

$$X(it+1) = X_{best} - r \cdot X_{rand} \cdot \cos\theta \quad (10)$$

$$X_{rand} = rand \cdot X_{best} - X_{current} \quad (11)$$

To make the searching and attacking structure proportional, a roulette wheel selection (R) was used. The R function is defined as equation (12). As the value of r_G getting smaller, the random value of R will also be reduced as well.

$$R = 2 \cdot r_G \cdot rand - r_G \quad (12)$$

When $|R| > 1$, the sand cats search or scout a new solution, diversely the sand cat assaults the prey. The balancing scheme of the proposed SCSO is useful for reaching rapid and accurate convergence points, making it suitable for finding the GMPP. The full flowchart of SCSO is illustrated in Figure 3.

Figure 3 shows that SCSO initiates the population at the first state, including the sand cat position, maximal iteration, and number of agents. Then, the initial position of the sand cat was ranked by their best fitness. The sand cat position is updated at each iteration loop based on their hunting mechanism using equation (7) and equation (10). Phase selection between searching and attacking is based on a Roulette

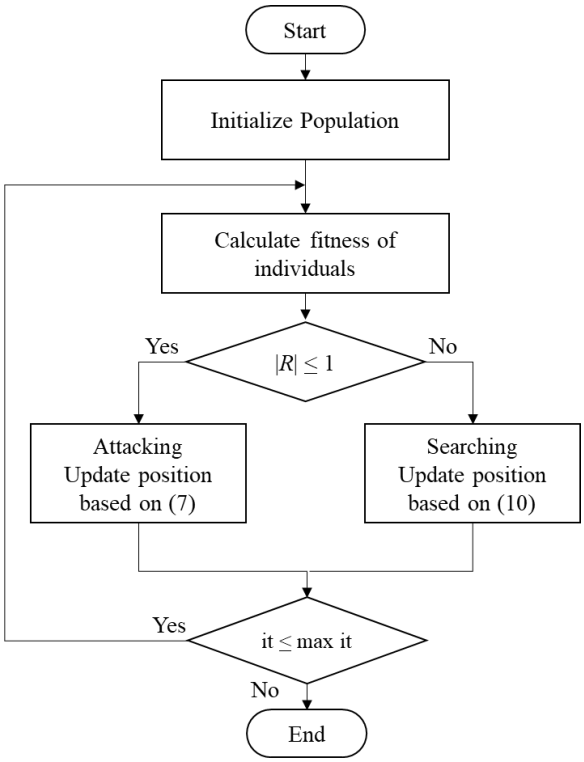

Figure 3. Flowchart of SCSO-MPPT.

Wheel selection (R). If $|R| \leq 1$, attacking phase equation (7) was run by the algorithm. Contrarily, if $|R| > 1$, the algorithm executes equation (10) as searching phase. After that, the solutions are assessed using a recalculated fitness function inside each iteration loop to identify the chameleon with the best fitness. The fittest solution is referred to as the best position of the chameleon that finds prey. All the steps in SCSO except the initialization step are repeated at each iteration until the maximum number of iterations is met. SCSO as the MPPT controller should achieve the GMPP state with swift movement and fewer oscillations. It leads the proposed system to boost the amount of energy harvested from the PV array.

III. Results and Discussions

A. Simulation test

In this section, the MPPT PV system is modeled and simulated using PSIM software. The proposed simulation model is shown in Figure 4. The circuit system consists of a series connection of five PV panels, a boost converter, an MPPT controller, and a resistive load. The performance effectiveness of the suggested SCSO-MPPT controller is assessed and contrasted with the performance of GWO, PSO, and tunicate swarm algorithm (TSA) algorithms. Table 3 states the parameter configurations of the algorithms. To maintain a fair execution of the test, several measures have been implemented. The quantity of particles

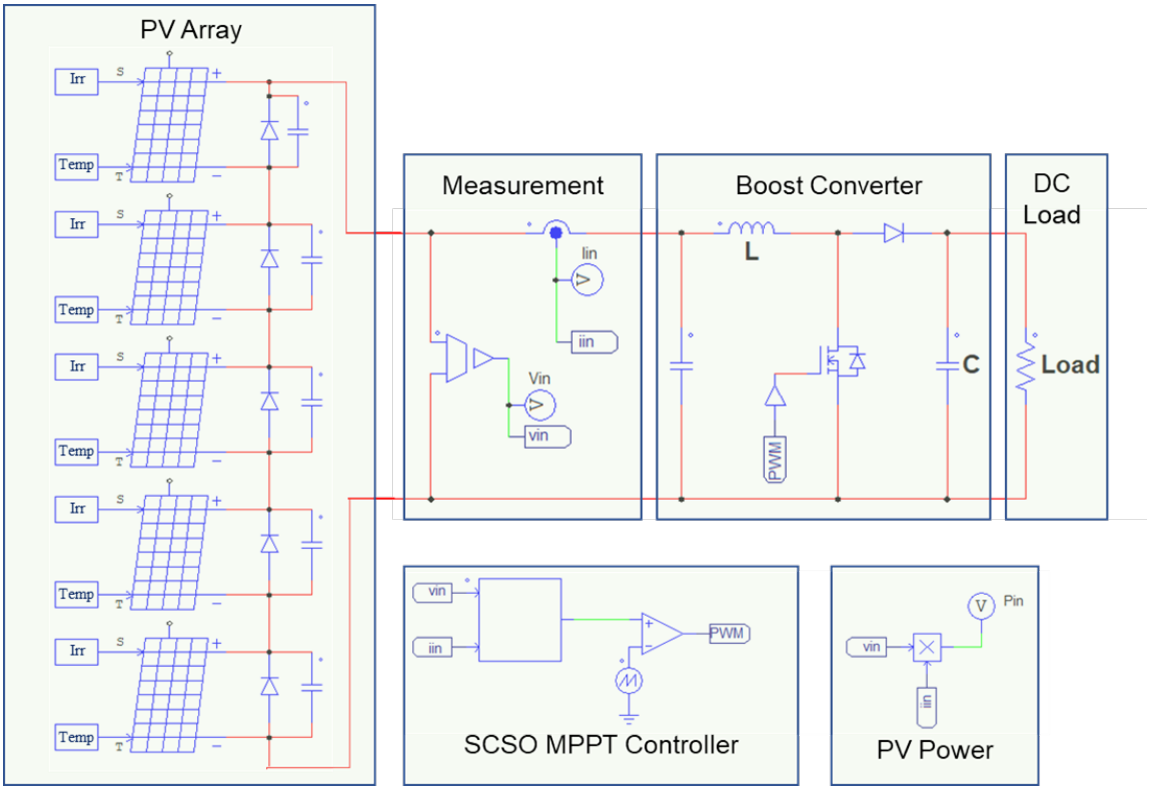

Figure 4. Proposed simulation model.

involved in the experiment has been restricted to 5, the upper limit for iterations has been set at 10, and all agents have been assigned an identical initial value.

The performance of the proposed SCSO is evaluated throughout two simulation assessments, including uniform conditions and partially shaded conditions. Table 4 presents the assortment of various patterns chosen for the PV system while retaining a constant temperature value of 25 C. The *P-V* characteristic of tested patterns is shown in Figure 5. Pattern 1 and pattern 2 are characterized by the uniform condition (UC), this condition only has one GMPP. The power peak of pattern 1 and pattern 2 are 500.2 W and 304.1 W, respectively. Pattern 3, pattern 4, and pattern 5 exhibit the partially shaded condition (PSC), which generates multiple peaks. There are four LMPPs in pattern 3 to pattern 5 and one GMPP, developed from 5-series PV panels. The GMPP of pattern 3 is 289.1 W, followed by pattern 4 at 228.9 W and pattern 5 at 202.9 W.

Pattern 1 displays a single peak of 500.3 W, as illustrated in Figure 5. The tracking waveforms produced by the four MPPT techniques in pattern 1 are shown in Figure 6. The proposed SCSO method adheres to the GMPP with a tracking accuracy of 99.98 % and an output power of 500.25 W in 2.25 s of tracking time. The PSO has demonstrated the highest accuracy of 99.99 % but at the cost of the longest tracking duration of 3.05 s. GWO and TSA exhibit significant oscillation as they approach convergence to the GMPP, with a tracking time of 2.95 s. The GWO has an output power of 499.48 W, whereas the TSA has an output power of 500.20 W. SCSO achieved the highest energy harvesting per 4 s simulation, followed by PSO, TSA, and GWO. Therefore, the SCSO approach exhibits the fastest tracking speed and yields the most captured energy.

Pattern 2 displays a single peak of 304.1 W, as illustrated in Figure 5. The tracking waveforms produced by the four MPPT techniques in the case of

Table 3.
Profile of algorithm parameters.

Algorithm	Parameter
SCSO	$S_M = 2$
GWO	$a = 2$ to $a = 0$
PSO	$w = 0.4; C_1 = 0.8; C_2 = 0.8$
TSA	$P_{max} = 4; P_{min} = 0$

Table 4.
Profile of irradiance for various patterns.

Pattern		Irradiance (W/m^2)					GMPP (W)
		PV 1	PV 2	PV 3	PV 4	PV 5	
1	UC	1000	1000	1000	1000	1000	500.3
2	UC	600	600	600	600	600	304.1
3	PSC	1200	500	800	600	700	289.1
4	PSC	500	1000	600	300	800	228.9
5	PSC	1100	300	400	600	800	202.9

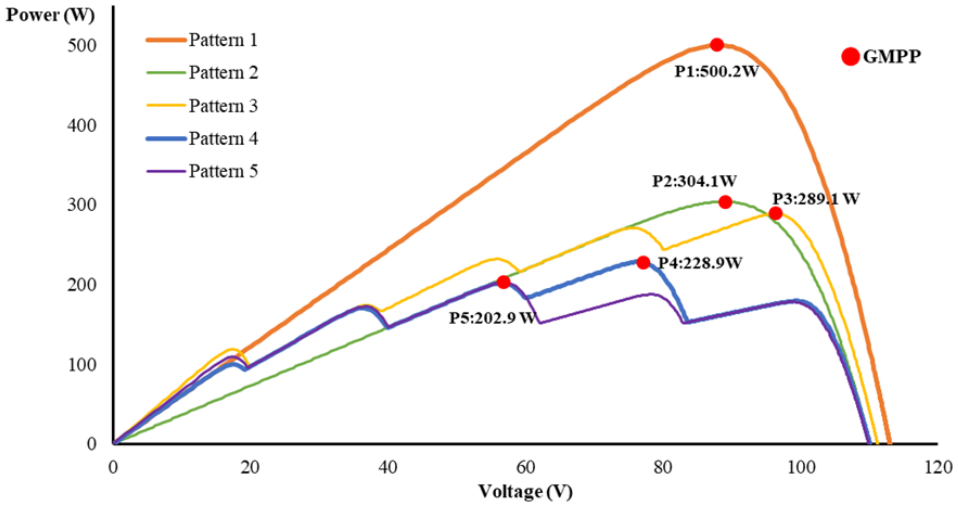

Figure 5. *P-V* characteristic of tested patterns.

pattern 2 are shown in Figure 7. The proposed SCSO method fits the GMPP with a tracking effectiveness of 99.99 %, a PV power of 304.03 W, and a rapid tracking time of 2.50 s. The PSO has a slow tracking duration of 3.05 s and achieves a tracking effectiveness of 99.60 %. Both the GWO and TSA approaches have a tracking time of 2.95 s, with tracking effectiveness of 99.97 % and 99.93 %, respectively. The pattern 2 simulation results show that the SCSO demonstrated the greatest quantity of harvested energy compared to other algorithms.

Figure 8 illustrates the tracking waveforms produced by the four MPPT techniques in pattern 3. Pattern 3 has four LMPPs and a GMPP of 289.1 W. The SCSO, as a proposed algorithm, effectively monitors the GMPP with a brief duration of 1 s and a tracking

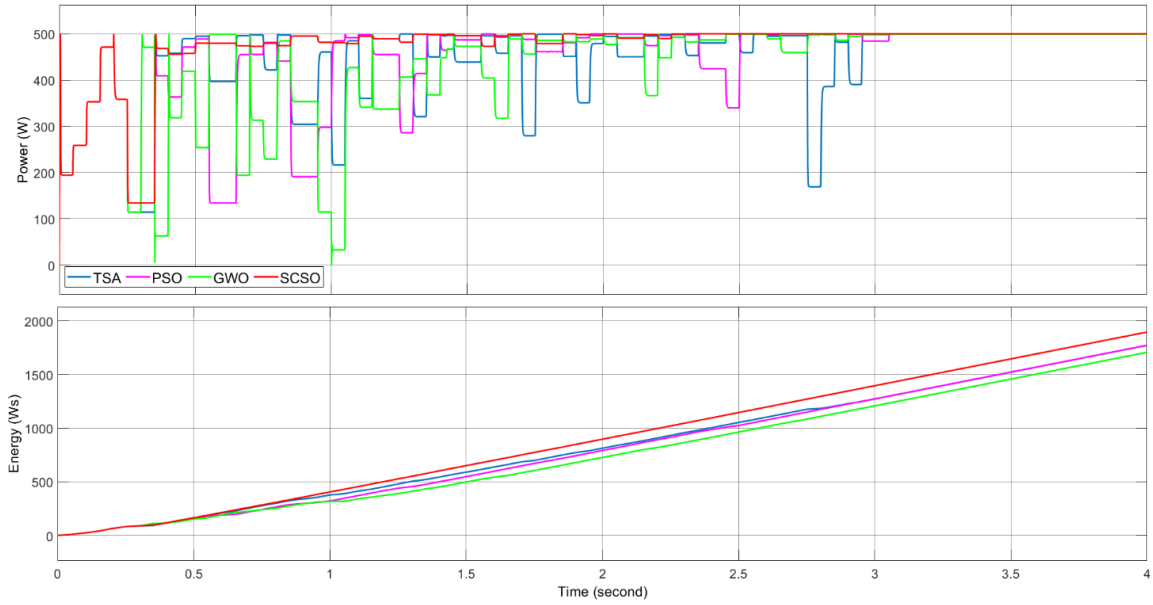

Figure 6. Result of pattern 1.

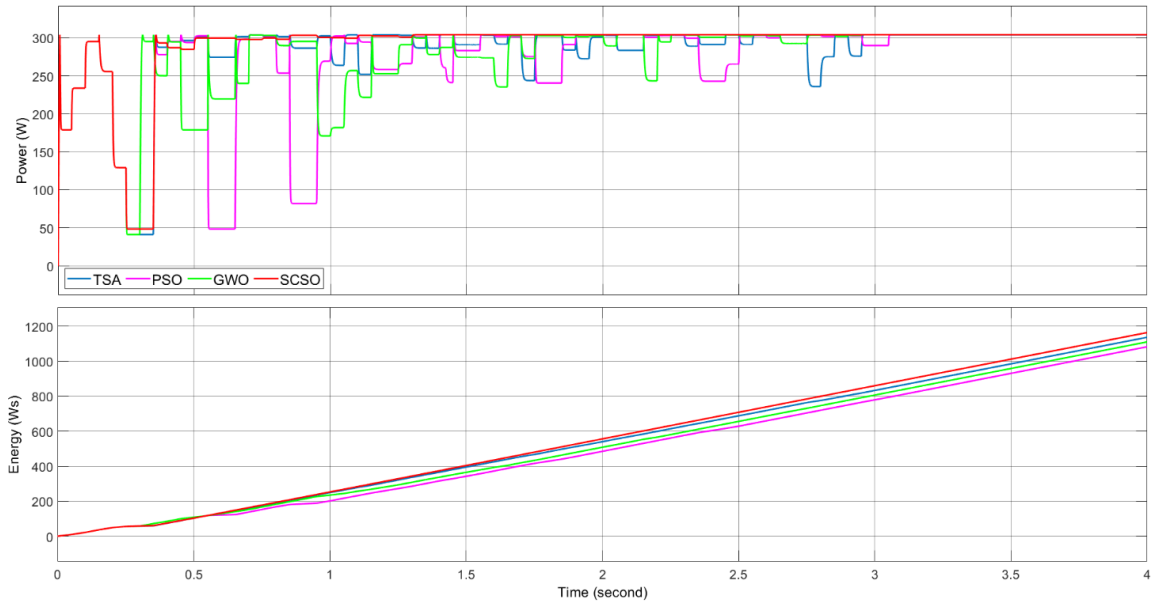

Figure 7. Result of pattern 2.

efficiency of 99.98 %. Additionally, it achieves a PV output power of 289.04 W. The GWO necessitates the longest tracking time of 3 s and exhibits a tracking efficiency of 99.97 %. PSO and TSA achieve convergence to the GMPP in a time frame of 2.95 s. The TSA has a tracking accuracy of 99.93 %, while the PSO has the lowest tracking accuracy at 99.60 %. Pattern 3 simulation results revealed that PSO achieved the lowest energy, while SCSO obtained the maximum energy.

Figure 9 exhibits the tracking waveforms produced by the four MPPT techniques in pattern 4. A GMPP of 228.9 W and the presence of four LMPPs occurred in pattern 4, as depicted in Figure 5. The SCSO approach, as a proposed algorithm, achieves convergence to the GMPP in a time of 2.45 s. Additionally, it demonstrates a tracking efficiency of 99.86 % and a PV power of 228.57 W. The GWO approaches the GMPP in 2.95 s, a longer duration than the previously discussed method. Additionally, it exhibits a tracking efficiency of 99.83 %. The PSO achieves a tracking efficiency of 99.27 % by accurately following the GMPP in 3.05 s, with a PV output power of 227.24 W. The TSA technique exhibits a tracking effectiveness of 99.83 % and a PV power of 228.50 W. As the simulation time was held in 4 s, the proposed SCSO demonstrated exceptional efficacy in enhancing the harvested energy from PV.

Pattern 5 has a GMPP of 202.9 W with the presence of four LMPPs, as illustrated in Figure 5. The tracking waveforms of pattern 5 depicted in Figure 10, are

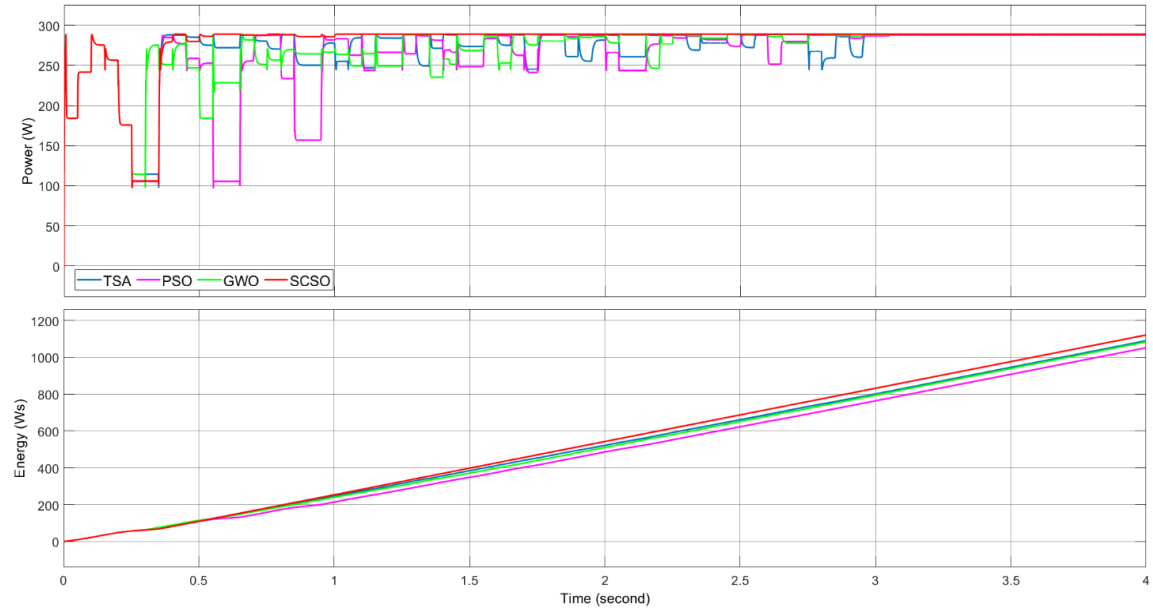

Figure 8. Result of pattern 3.

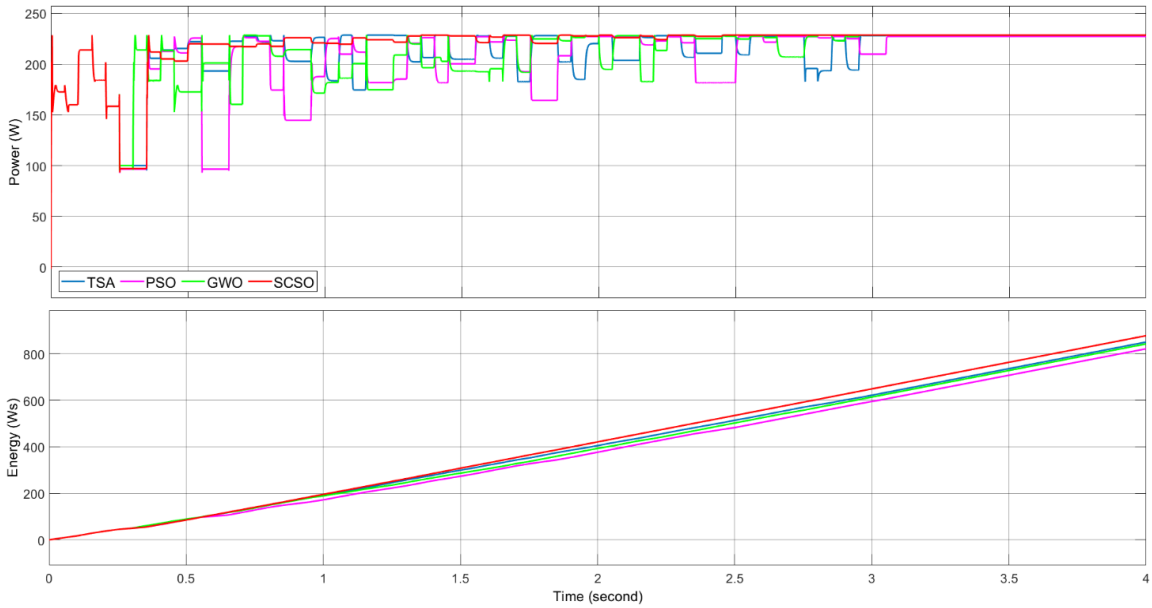

Figure 9. Result of pattern 4.

produced by the four MPPT approaches. SCSO, the proposed algorithm, succeeds in convergence to the GMPP in a period of 1.85 s. It demonstrates a tracking efficiency of 99.90 % and a PV output power of 202.68 W. The PSO algorithm achieves the GMPP in 3.05 s, the maximum tracking time. It exhibits a tracking efficiency of 99.86 %. The TSA achieves a tracking efficiency of 99.34 % by tracking the GMPP in 2.95 s, with a PV output power of 201.57 W. Nevertheless, the GWO technique encounters an obstacle at LMPP. The tracking efficiency is 92.40 %, and the PV output power is 187.48 W. SCSO achieved the highest level of energy collection from PV, followed by TSA, PSO, and GWO.

The tracking graphs depicted in Figure 6 to Figure 10 demonstrate that while both PSO and TSA provide global convergence, they require a lengthy duration. Furthermore, power fluctuations appeared in TSA and PSO for a more extended period. It results in a substantial decrease in collected energy. Also, the GWO algorithm expresses a lengthy period of converging and is incapable of identifying the GMPP at pattern 5. By the simulation results shown in Figure 6 to Figure 10, the SCSO method demonstrates superior performance compared to the GWO, PSO, and TSA methods regarding faster convergence to GMPP, slight power oscillations, and more tremendous harvested energy. This demonstrates the SCSO's ability to handle any atmospheric conditions proficiently. Table 5 presents an overview of the simulation findings. The SCSO-MPPT method surpasses the other three existing

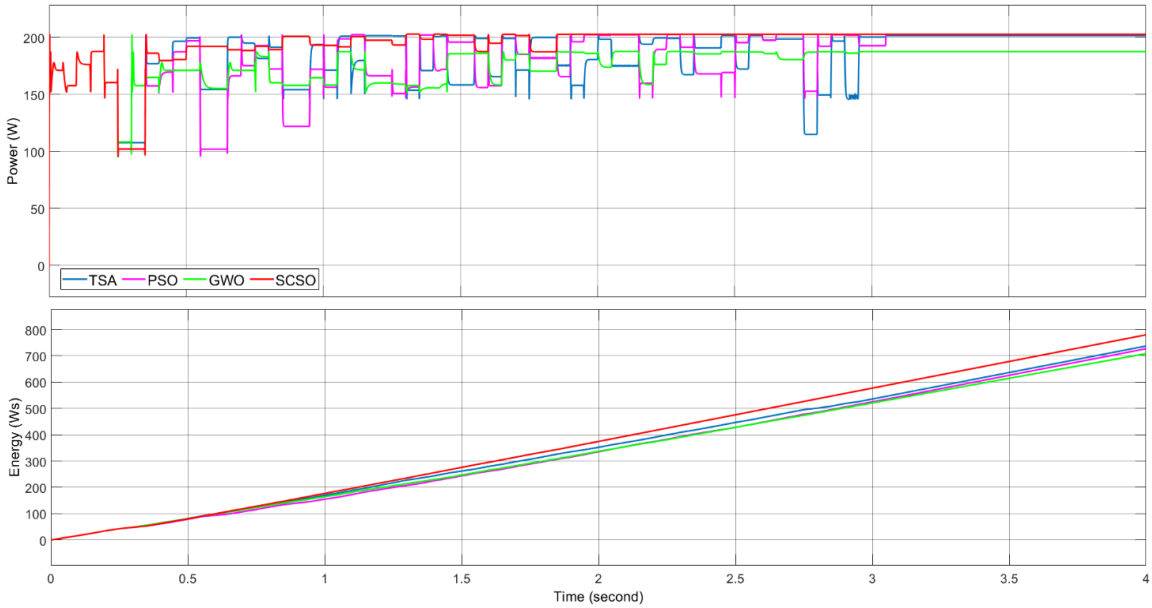

Figure 10. Result of pattern 5.

Table 5.
Simulation results data.

Pattern	Algorithm	Power output (W)	Tracking time (s)	Tracking accuracy (%)	Energy (W·s)
1	SCSO	500.25	2.25	99.98	1896.17
	GWO	499.48	2.95	99.84	1709.57
	PSO	500.28	3.05	99.99	1773.11
	TSA	500.20	2.95	99.98	1772.70
2	SCSO	304.03	1.35	99.99	1163.11
	GWO	304.02	2.95	99.99	1110.56
	PSO	303.93	3.05	99.96	1083.66
	TSA	303.84	2.95	99.93	1137.91
3	SCSO	289.04	1.00	99.98	1120.76
	GWO	289.02	3.00	99.97	1083.35
	PSO	287.94	2.95	99.60	1055.42
	TSA	288.90	2.95	99.93	1089.80
4	SCSO	228.57	2.45	99.86	877.36
	GWO	228.50	2.95	99.83	841.98
	PSO	227.24	3.05	99.27	825.55
	TSA	228.50	3.05	99.83	850.11
5	SCSO	202.68	1.85	99.90	779.73
	GWO	187.48	2.95	92.40	708.18
	PSO	202.62	3.05	99.86	726.47
	TSA	201.57	2.95	99.34	740.31

Table 6.
Result of Friedmann rank test.

Pattern	Rank at 1	Rank at 2	Rank at 3	Rank at 4	Rank at 5	Overall rank
SCSO	1.33	1.00	1.00	1.00	1.00	1
GWO	3.20	2.18	2.53	2.18	3.20	3
PSO	1.45	3.43	3.20	4.00	2.53	4
TSA	2.67	2.67	2.40	2.29	2.67	2

MPPT methods, with an average value of 99.94 % tracking accuracy and 1.78 s tracking time. Thus, the SCSO demonstrated exceptional efficiency in enhancing the harvested energy from PV.

A comprehensive analysis is conducted to compare the SCSO technique with other methods created in the implementation of MPPT. The aim is to comprehend better the impact of the SCSO method on the application of MPPT. The Friedman ranking test was conducted to determine the comparative rank of the suggested algorithm within the overall ranks. Table 6 contains the conclusions of the Friedman ranking test. Among algorithms tested for GMPP tracking under various patterns, the proposed SCSO emerged as the most superior algorithm, followed by TSA, GWO, and PSO.

B. Experimental test

The experimental prototypes for this study are photographed in Figure 11. It consists of a solar PV

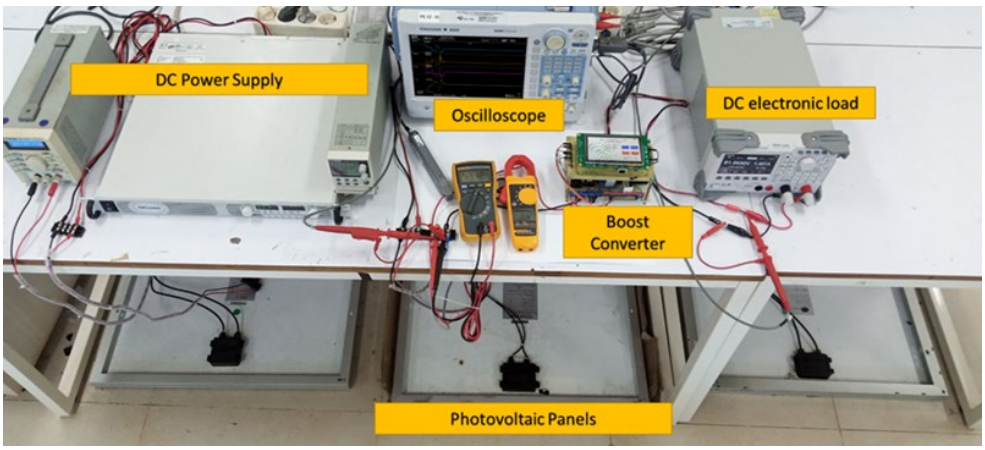

Figure 11. Experimental prototype.

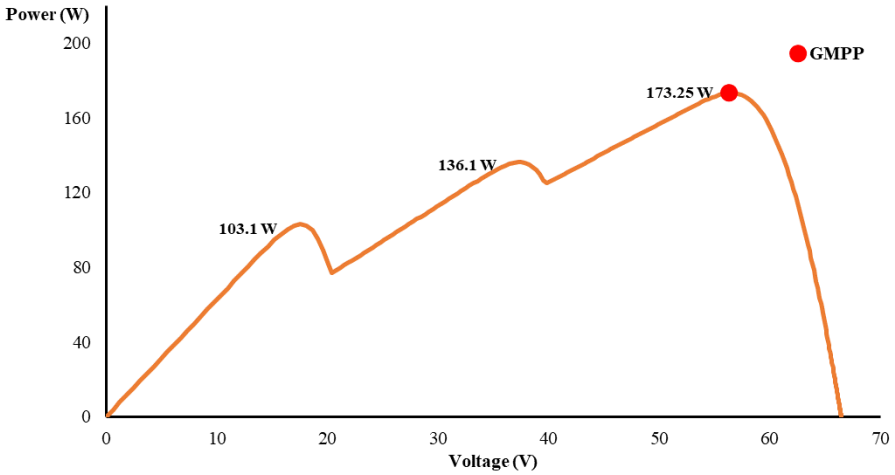

Figure 12. *P-V* characteristic of the experimental test.

emulator, oscilloscope, boost converter, and DC electronic load. The partial shading condition was emulated using an unilluminated solar PV technique by 3-series 100 Wp PV panels and DC power supply as the solar PV emulator. The PV panels should be oriented in a downward position to avoid direct exposure to solar irradiation. Subsequently, the current source for the PV panel is substituted with the DC power supply. With the unilluminated solar PV technology, the irradiation value on the PV panel can be regulated by adjusting the DC power supply. The oscilloscope is recorded in the tracking process of MPPT. DC electronic load is operated as a constant resistive load. For the experimental test, it needed to change the sampling time for measuring PV output voltage and current. It is used to achieve precise measurements of the PV output. Therefore, the simulation utilized a sample time of 0.05 s, while the experiment employed a sampling time of 0.5 s.

The proposed SCSO-MPPT performance was examined under partially shaded conditions, with the irradiation values are 600 W/m^2, 500 W/m^2, and 1000 W/m^2. It exhibits a maximum power of 173.25 W, with the voltage and current being 56.62 V and 3.06 A respectively. The *P-V* characteristic of the experimental test is shown in Figure 12.

Figure 13 shows the performance of SCSO with a maximum power of 172.23 W and a tracking duration

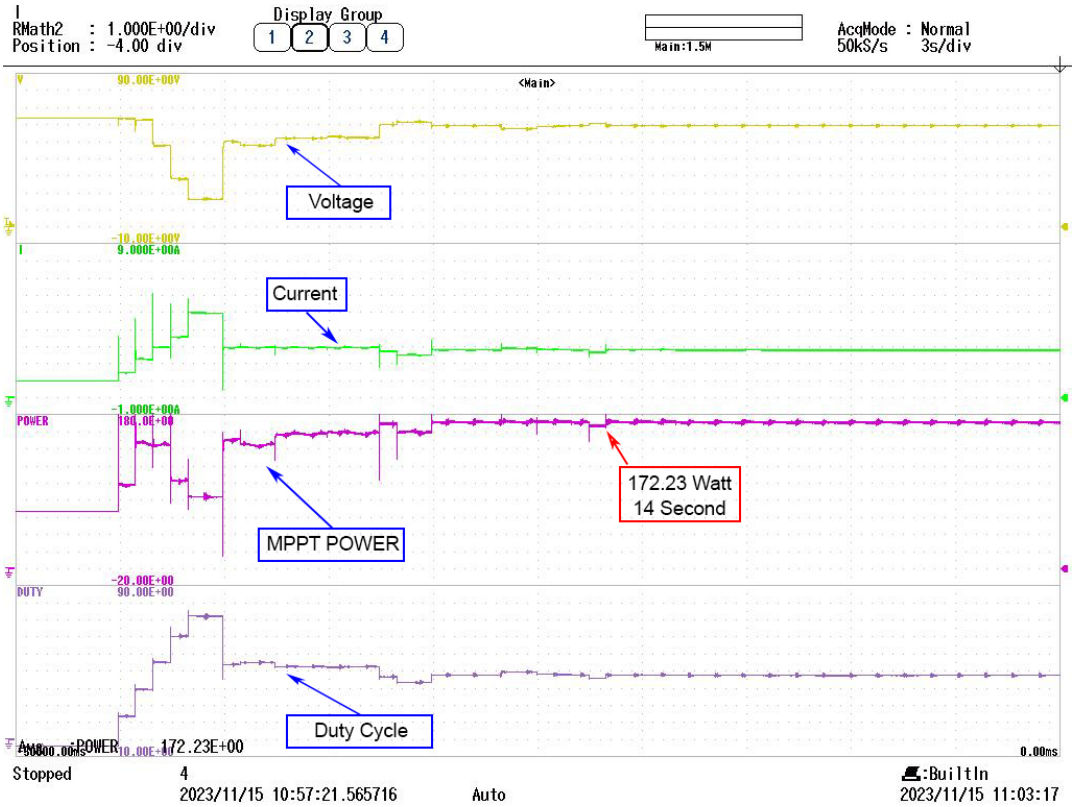

Figure 13. MPPT experimental result of SCSO-MPPT.

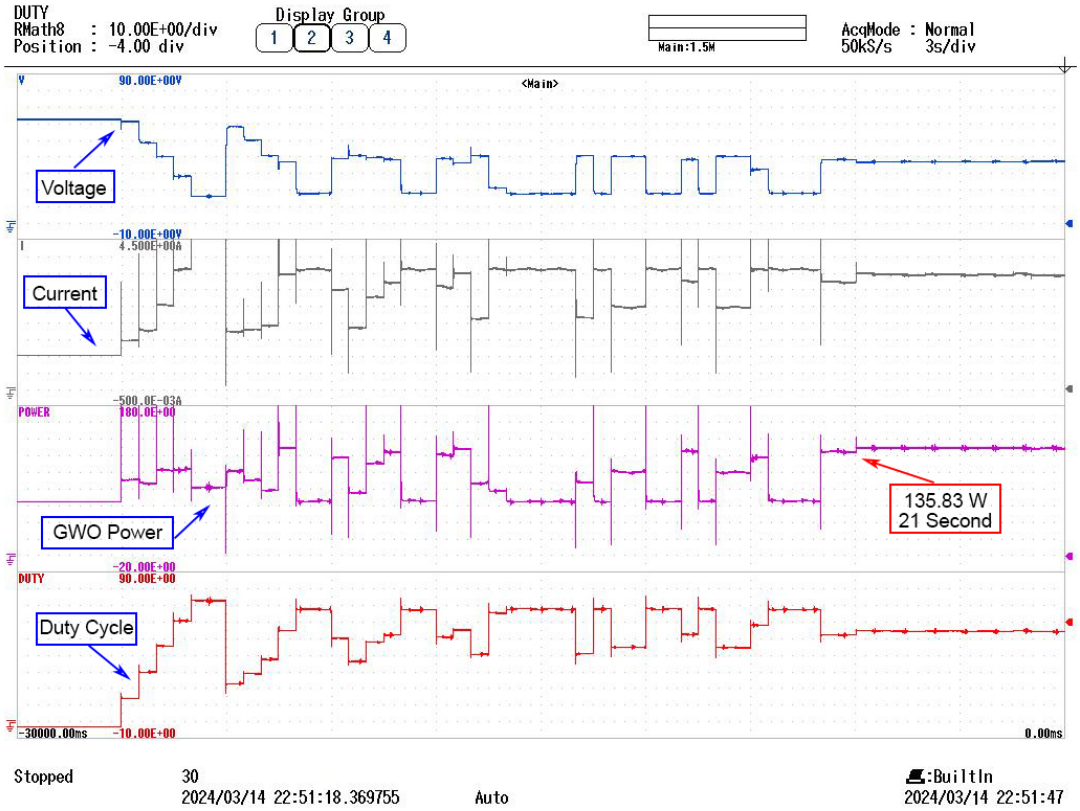

Figure 14. MPPT experimental result of GWO-MPPT.

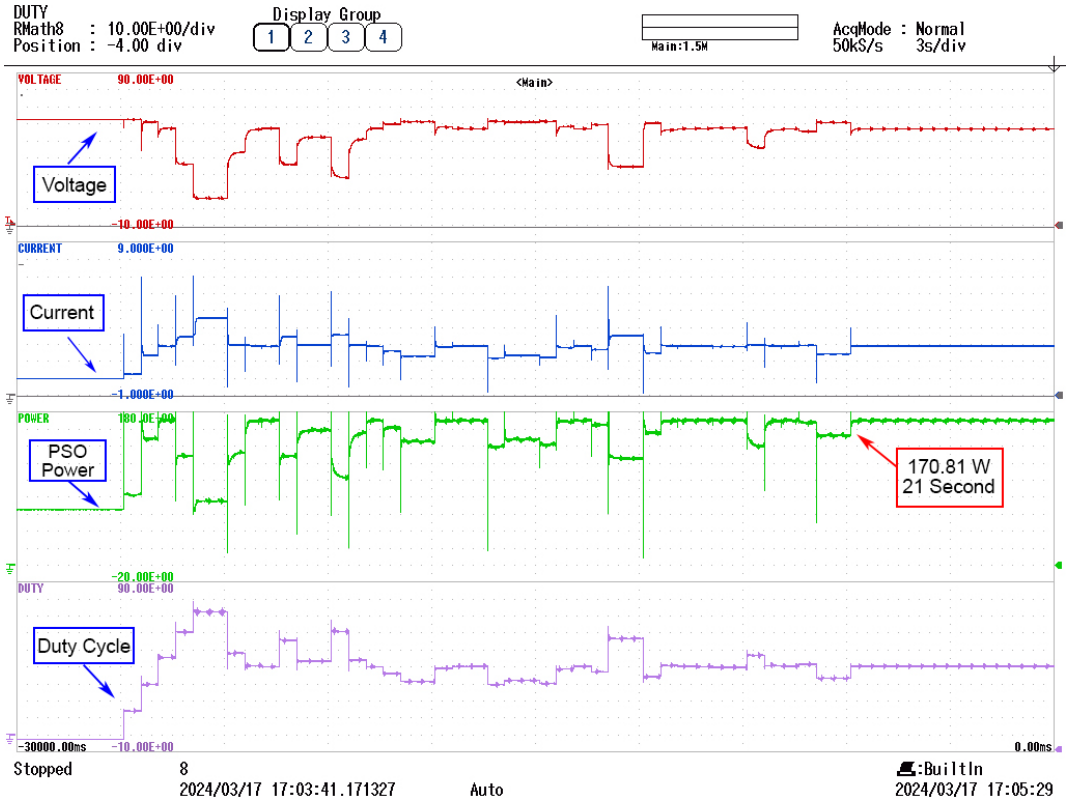

Figure 15. MPPT experimental result of PSO-MPPT.

of 14 s. The proposed SCSO-MPPT succeeded in securing the GMPP at a precision rate of 99.4 %, with the values of voltage, current, and duty cycle are 58.79 V, 2.93 A, and 38 % respectively. Figure 14 to Figure 16 show the performance of the compared algorithm. The tracking performance of GWO is shown in Figure 14 with a maximum power of 135.83 W and a tracking duration of 21 s. Figure 15 shows the performance of PSO in getting GMPP with a maximum power of 170.81 W and a tracking duration of 21 s. Figure 16

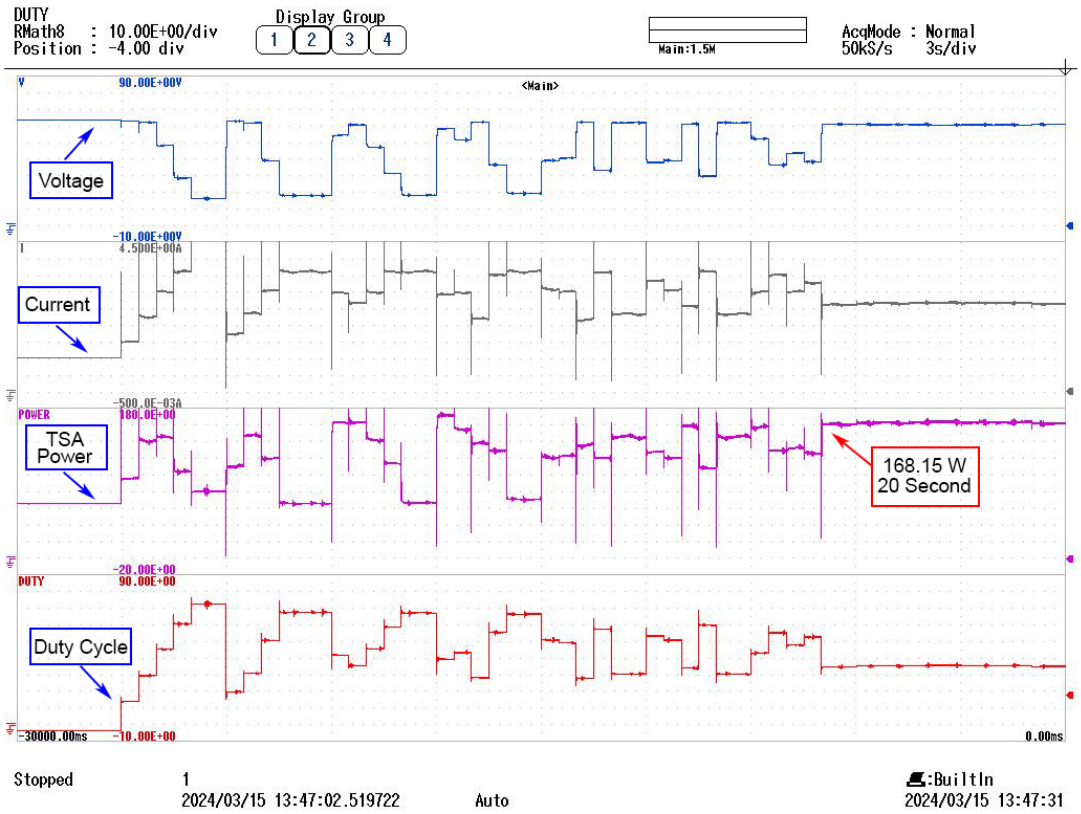

Figure 16. MPPT experimental result of TSA-MPPT.

shown the performance of TSA with a maximum power of 168.15 W and a tracking duration of 20 s. The tracking diagrams illustrate that both PSO and TSA exhibit GMPP convergence, though with a long time period. In addition, PSO and TSA suffered power fluctuations over a longer duration. Moreover, GWO exhibits a protracted convergence period and fails to detect the GMPP. Regarding the experimental results depicted in Figure 13 to Figure 16, the SCSO technique exhibits superior performance in terms of faster convergence to GMPP, higher output power, and less power oscillations when compared to the GWO, PSO, and TSA methods. The experimental test results show that the proposed algorithm, SCSO, demonstrates the capability to effectively address partially shaded conditions in real-world scenarios with an optimal performance.

IV. Conclusion

This article introduces a SCSO-MPPT algorithm, inspired by the biological phenomena of sand cat. It is designed to optimize power extraction and enhance harvested energy from PV systems across diverse weather conditions. The SCSO algorithm undergoes rigorous testing, initially in two conditions of uniform irradiance. Subsequently, its performance is evaluated under three distinct partially shaded conditions. In uniform conditions, the SCSO method exhibits high tracking accuracy, averaging 99.98 %, with a shorter tracking time. Additionally, an average accuracy of 99.92 % is reported under PSC. Overall, SCSO has a tracking accuracy rate of 99.94 % with quicker tracking time and minor oscillation. The SCSO algorithm distinguishes between local and global peaks, even in the presence of shadows. Comparative analyses with other bio-inspired methods consistently position SCSO at the forefront. Friedman rank tests further confirm SCSO's significant superiority over other evaluated MPPT methods. SCSO was ranked in the top place, followed by TSA, GWO, and PSO. Despite these successes, the proposed SCSO MPPT algorithm exhibits limitations, particularly challenges in parameter initialization. The remarkable results from the SCSO-MPPT technique underscore its efficacy and superiority in enhancing the optimal power of PV systems, especially when prioritizing in energy harvesting.

Acknowledgements

The authors would like to express our gratitude to Politeknik Elektronika Negeri Surabaya (PENS) and Green Electrification Laboratory for granting permission to utilize the hardware tools in this research, as well as to those individuals who have provided assistance and support in the preparation of this manuscript.

Declarations

Author contribution

M.R.D. Abdilla: Writing - Original Draft, Writing - Review & Editing, Conceptualization, Formal analysis, Software, Hardware, Investigation, Visualization. **N.A. Windarko**: Writing - Review & Editing, Investigation, Validation, Supervision. **B. Sumantri**: Formal analysis, Investigation, Validation, Supervision.

Funding statement

This research did not receive any specific grant from funding agencies in the public, commercial, or not-for-profit sectors.

Competing interest

The authors declare that they have no known competing financial interests or personal relationships that could have appeared to influence the work reported in this paper.

Additional information

Reprints and permission: information is available at https://mev.brin.go.id/.

Publisher's Note: National Research and Innovation Agency (BRIN) remains neutral with regard to jurisdictional claims in published maps and institutional affiliations.

References

[1] R. Ahmed, V. Sreeram, Y. Mishra, and M. D. Arif, "A review and evaluation of the state-of-the-art in PV solar power forecasting: Techniques and optimization," *Renewable and Sustainable Energy Reviews*, vol. 124, no. February, p. 109792, 2020.

[2] M. B. Hayat, D. Ali, K. C. Monyake, L. Alagha, and N. Ahmed, "Solar energy—A look into power generation, challenges, and a solar-powered future," *International Journal of Energy Research*, vol. 43, no. 3, pp. 1049–1067, 2019.

[3] M. Qaraad, S. Amjad, N. K. Hussein, M. Badawy, S. Mirjalili, and M. A. Elhosseini, "Photovoltaic parameter estimation using improved moth flame algorithms with local escape operators," *Computers and Electrical Engineering*, vol. 106, no. September 2022, p. 108603, 2023.

[4] M. Padmanaban, S. Chinnathambi, P. Parthasarathy, and N. Pachaivannan, "An Extensive Study on Online, Offline and Hybrid MPPT Algorithms for Photovoltaic Systems," *Majlesi Journal of Electrical Engineering*, vol. 15, no. 3, pp. 1–16, 2021.

[5] P. K. Bonthagorla and S. Mikkili, "Performance analysis of PV array configurations (SP, BL, HC and TT) to enhance maximum power under non-uniform shading conditions," *Engineering Reports*, vol. 2, no. 8, 2020.

[6] G. Abdullah, H. Nishimura, and T. Fujita, "An experimental investigation on photovoltaic array power output affected by the different partial shading conditions," *Energies*, vol. 14, no. 9, 2021.

[7] K. Lappalainen and S. Valkealahti, "Number of maximum power points in photovoltaic arrays during partial shading events by clouds," *Renewable Energy*, vol. 152, pp. 812–822, 2020.

[8] J. Li, Y. Wu, S. Ma, M. Chen, B. Zhang, and B. Jiang, "Analysis of photovoltaic array maximum power point tracking under uniform environment and partial shading condition: A review," *Energy Reports*, vol. 8, pp. 13235–13252, 2022.

[9] D. Sera, L. Mathe, T. Kerekes, S. V. Spataru, and R. Teodorescu, "On the perturb-and-observe and incremental conductance mppt methods for PV systems," *IEEE Journal of Photovoltaics*, vol. 3, no. 3, pp. 1070–1078, 2013.

[10] N. F. M. Yusof, D. Ishak, and M. Salem, "An Improved Control Strategy for Single-Phase Single-Stage Grid-Tied PV System Based on Incremental Conductance MPPT, Modified PQ Theory, and Hysteresis Current Control," *Engineering Proceedings*, vol. 12, no. 1, pp. 10–13, 2022.

[11] V. Jately, B. Azzopardi, J. Joshi, B. Venkateswaran V, A. Sharma, and S. Arora, "Experimental Analysis of hill-climbing MPPT algorithms under low irradiance levels," *Renewable and Sustainable Energy Reviews*, vol. 150, p. 111467, 2021.

[12] S. Mahmoodi Tabar, M. Shahnazari, and K. Heshmati, "Maximum power point tracking in partially shaded photovoltaic systems using grasshopper optimization algorithm," *IET Renewable Power Generation*, vol. 17, no. 2, pp. 389–399, 2023.

[13] L. Bhukya, N. R. Kedika, and S. R. Salkuti, "Enhanced Maximum Power Point Techniques for Solar Photovoltaic System under Uniform Insolation and Partial Shading Conditions: A Review," *Algorithms*, vol. 15, no. 10, 2022.

[14] A. S. Pawar, M. T. Kolte, and H. Mehta, "Review of PV MPPT Based Battery Charging Techniques under Partial Shading Conditions," *ICPC2T 2022 - 2nd International Conference on Power, Control and Computing Technologies, Proceedings*, 2022.

[15] R. B. A. Koad, A. F. Zobaa, and A. El-Shahat, "A Novel MPPT Algorithm Based on Particle Swarm Optimization for Photovoltaic Systems," *IEEE Transactions on Sustainable Energy*, vol. 8, no. 2, pp. 468–476, 2017.

[16] A. I. Nusaif and A. L. Mahmood, "MPPT Algorithms (PSO, FA, and MFA) for PV System Under Partial Shading Condition, Case Study: BTS in Algazalia, Baghdad," *International Journal of Smart grid*, no. September, 2020.

[17] J. Aguila-Leon, C. Vargas-Salgado, C. Chiñas-Palacios, and D. Díaz-Bello, "Solar photovoltaic Maximum Power Point Tracking controller optimization using Grey Wolf Optimizer: A performance comparison between bio-

inspired and traditional algorithms," *Expert Systems with Applications*, vol. 211, 2023.

[18] M. J. Alshareef, "An Effective Falcon Optimization Algorithm Based MPPT Under Partial Shaded Photovoltaic Systems," *IEEE Access*, vol. 10, pp. 131345–131360, 2022.

[19] E. H. de Vasconcelos Segundo, V. C. Mariani, and L. dos S. Coelho, "Design of heat exchangers using Falcon Optimization Algorithm," *Applied Thermal Engineering*, vol. 156, no. April, pp. 119–144, 2019.

[20] E. N. Sholikhah, N. A. Windarko, and B. Sumantri, "Tunicate swarm algorithm based maximum power point tracking for photovoltaic system under non-uniform irradiation," *International Journal of Electrical and Computer Engineering*, vol. 12, no. 5, pp. 4559–4570, 2022.

[21] N. Douifi, A. Abbadi, F. Hamidia, K. Yahya, M. Mohamed, and N. Rai, "A Novel MPPT Based Reptile Search Algorithm for Photovoltaic System under Various Conditions," *Applied Sciences (Switzerland)*, vol. 13, no. 8, 2023.

[22] Y. Li and G. Wang, "Sand Cat Swarm Optimization Based on Stochastic Variation With Elite Collaboration," *IEEE Access*, vol. 10, pp. 89989–90003, 2022.

[23] L. Guo, Z. Meng, Y. Sun, and L. Wang, "A modified cat swarm optimization based maximum power point tracking method for photovoltaic system under partially shaded condition," *Energy*, vol. 144, pp. 501–514, 2018.

[24] X. Wang, Q. Liu, and L. Zhang, "An Adaptive Sand Cat Swarm Algorithm Based on Cauchy Mutation and Optimal Neighborhood Disturbance Strategy," *Biomimetics*, vol. 8, no. 2, p. 191, May 2023.

[25] G. Xiong, L. Li, A. W. Mohamed, X. Yuan, and J. Zhang, "A new method for parameter extraction of solar photovoltaic models using gaining–sharing knowledge based algorithm," *Energy Reports*, vol. 7, pp. 3286–3301, 2021.

[26] M. Z. Aihsan, N. I. Ahmad, W. A. Mustafa, N. A. Rahman, and J. A. Soo, "Development of square wave inverter using DC/DC boost converter," *International Journal of Power Electronics and Drive Systems*, vol. 10, no. 2, pp. 636–644, 2019.

[27] A. Seyyedabbasi and F. Kiani, "Sand Cat swarm optimization: a nature-inspired algorithm to solve global optimization problems," *Engineering with Computers*, no. April, 2022.